Application of a Fiber-Matrix Model to Transport in Renal Tubules

W. D. FRASER and A. D. BAINES

From the Toronto General Hospital, ES 3-404D, Toronto, Ontario M5G 2C4, Canada

ABSTRACT The effects of tight junction structure on water and solute fluxes across proximal tubular epithelium were examined with fiber-matrix equations previously derived by Curry and Michel (1980. *Microvascular Research.* 20:96–99). Using plausible estimates of tight junction fiber length and width the model predicts solute (P_S) and water permeability (L_p) coefficients that agree with the measured values. When fiber-matrix and pore models were compared for physiologically relevant ranges of matrix void fraction (80–98%) and pore radii (0–20 Å), the fiber-matrix model predicted a 10-fold higher L_p/P_s ratio. L_p/P_s was most sensitive to small changes in tight junction structure when void fractions exceeded 90%. Void fractions of 96.5% and 97.1% predicted previously measured values for L_p and solute permeabilities in rat and rabbit proximal tubules. These values are consistent with void fractions and permeabilities of artificial membranes. The fiber-matrix tight junction model was incorporated into a model of reabsorption from the rat proximal tubule developed by Weinstein (1984. *American Journal of Physiology.* 247:F848-F862.) A void fraction of 98% predicted the experimental results for isosomotic reabsorption driven by active transport. Changing void fraction over the range of 97–99% produced a 50–75% change in predicted volume reabsorption with active transport. According to the fiber-matrix model: (*a*) solute permeabilities alone cannot be used to predict L_p, (*b*) previously measured solute permeabilities in the proximal tubule are compatible with significant water reabsorption through a water-permeable tight junction, and (*c*) hydraulic and solute permeabilities may be sensitive to small changes in tight junction fiber length and diameter or ionic strength within the tight junction.

INTRODUCTION

In this paper we describe the application of a fiber-matrix model to the question of paracellular fluid and solute transport in the proximal tubule. The relative importance of paracellular and transcellular pathways for water reabsorption is unresolved (Diamond, 1979). Preisig and Berry (1985) argued that the pore size and area of the tight junction are too small for there to be significant flow through the paracellular pathway in proximal tubules. In their analysis, using the Pappenheimer pore model (Pappenheimer et al., 1951), they estimated pore dimensions from the permeabilities of lipophobic nonelectrolytes (Preisig and Berry, 1985). Since the

Address reprint requests to Dr. A. D. Baines, Department of Clinical Biochemistry, Toronto General Hospital, ES 3-404D, 200 Elizabeth Street, Toronto, Ontario, Canada M5G 2C4.

J. GEN. PHYSIOL. © The Rockefeller University Press · 0022-1295/89/11/0863/17 $2.00
Volume 94 November 1989 863–879

hydraulic permeability of the tight junction calculated using this pore model was less than the experimentally measured values for proximal tubules they concluded that tight junctions cannot be the primary route for transepithelial fluid movement.

According to Preisig and Berry (1985), the inapplicability of Poiseuille's equation to very small pores forces one to conclude that the movement of water across tight junctions is strictly diffusive. However, as will be shown below, theoretical arguments indicate that Poiseuille's equation underestimates flow through fiber-matrix membranes. This fact has been confirmed experimentally by showing that pore models underestimate bulk fluid flow and diffusion through ultraporous membranes (Yasuda et al., 1971), cartilage (Maroudas, 1970), and the junctions between endothelial cells (Curry and Michel, 1980).

A recent review of the structure, biochemistry, and assembly of epithelial tight junctions summarizes the limited knowledge of the structure (Gumbiner, 1987). Freeze-fracture shows the tight junctions as a belt-like set of strands, running parallel to the luminal surface, which may be likened to a set of o-rings making up the seal surrounding a rotating shaft. Internally the strands are believed to be made up of a glycoprotein mesh cross-linked by calcium and linked to carbohydrate moieties bound to the membranes of the adjoining cells (Hayward and Hackemann, 1973; Oschman, 1978; Griepp et al., 1983). It is these attachment sites that one observes in freeze-fracture micrographs of the tight junctions (Gumbiner, 1987). The functional properties of the tight junction appear to be related to both the structure and the number of strands. For the most part the strands run parallel to the epithelial surface, so the number of strands will determine the effective thickness of the tight junction. The hydraulic and solute permeabilities of the tight junction are thus determined by both the internal composition of the strands and the number of strands. However, one cannot determine the detailed structure of the proteins making up the tight junction strands from the freeze-fracture images (Gumbiner, 1987).

Movement of solutes through such a protein mesh may be described by paraphrasing the description of Yasuda et al. (1971) for water-swollen polymer membranes. They visualize that pores or channels in the membrane are mobile in size and location and that the size and shape of these solvent-filled pores change continuously. The geometry of the polymer network sets the upper limit for the size and shape of permeating molecules and passage through the membrane depends on the probability that the permeant molecule finds at its location a suitable hole. The pores of this concept are described as "the 'free-volume element' since the total amount of such pores or channels in a unit volume of the membrane represents the ratio of free volume accessible to the transport of the permeant" (Yasuda et al., 1971). This concept of the fiber-matrix membrane has been used by Curry and Michel (1980) and independently by Yasuda et al. (1971) to describe volume and solute fluxes throught the intercellular gap between endothelial cells and across artificial porous membranes. In this model the equations for hydraulic permeability coefficient (L_p), the solute permeability coefficient (P_s), and the solute reflection coefficient (σ), show a remarkable consistency in that, once one of these transport coefficients has been determined the other two transport coefficients fit the experimental data for capillary endothelium.

EQUATIONS

The combined set of equations to describe solute and volume flow across a fiber-matrix membrane was developed by Curry (1980) and Curry and Michel (1980) from the work of Ogston et al. (1973) on solute permeability, and Kozeny (1927) on hydraulic permeability. Essentially identical expressions were independently developed by Yasuda et al. (1971). The approach used to describe the solute permeability for a fiber-matrix membrane is based on the conventional expression for solute permeability in homogenerous nonporous membranes, where the solute permeability is a function of the solute diffusivity in the membrane, D_m, and the solute partition coefficient for the membrane-bathing solution interface, K:

$$P_s = \frac{D_m K}{\Delta x}, \tag{1}$$

where Δx is the membrane thickness. From Curry and Michel (1980) one can obtain equations describing both the solute diffusivity, D_m, in the fiber matrix as well as the solute partition coefficient K, i.e.,

$$K = \exp\left\{-(1-\epsilon)\left[\left(\frac{2a}{r_f}\right) + \left(\frac{a}{r_f}\right)^2\right]\right\}, \tag{2}$$

and

$$D_m = D_0 \exp\left[-(1-\epsilon)^{0.5}\left(1 + \frac{a}{r_f}\right)\right], \tag{3}$$

where D_0 is the solute diffusivity in the bulk medium, ϵ is the void fraction of the membrane, a is the solute radius, and r_f is the fiber radius. The void fraction can be expressed as a function of the fiber radius, r_f, and the length of the fiber per unit volume of fiber matrix, l:

$$\epsilon = (1 - \pi r_f^2 l). \tag{4}$$

Curry and Michel (1980) used these expressions for K and D_m in the conventional permeability expression along with a term for the fractional area of the total epithelium composed of the permeable matrix, A_f, to arrive at an expression describing the permeability coefficient for the total epithelium:

$$P_s = \frac{A_f D_0 \exp\left[-\pi^{0.5} l^{0.5}(a + r_f) - \pi l(2ar_f + a^2)\right]}{\Delta x}. \tag{5}$$

The corresponding equation for the pore model is

$$P_s = \frac{N_p \pi r_p^2 D_0 (1 - a/r_p)^2}{\Delta x} \tag{6}$$

in which for the case of cylindrical pores $(1 - a/r_p)^2$ is the steric exclusion factor to account for the interaction of the solute with the pore walls having radius r_p (Curry, 1984). N_p is the number of pores in the membrane.

For volume flow through the fiber matrix Curry and Michel (1980) used the Carmen-Kozeny equation (Bear, 1972; Massey, 1983) originally developed to describe

fluid flow through random arrays of macroscopic fibers, but applicable to the microscopic mesh of gel-like structures. The expression for the hydraulic permeability (normalized to the total membrane area) is

$$L_p = \frac{A_f \epsilon^3 r_f^2}{\Delta x (1 - \epsilon)^2 4\kappa\eta}, \tag{7}$$

where η is the bulk fluid phase viscosity, and κ is the Kozeny constant, which is a function of the "tortuosity" and shape of the membrane channels. κ has been experimentally shown to vary from 2.0 to 6.0 (Adamson and Curry, 1982) for a large variety of porous structures (Carman, 1937; Curry and Michel, 1980), but reaches values of 13.0 for calcined alumina membranes in which the fibers are arranged parallel to the membrane surface (Leenaars and Burggraaf, 1985). For hyaluronic acid gels of very high void fraction, κ has been found to have a value of 2.0 (Adamson and Curry, 1982).

The corresponding expression for the pore model is

$$L_p = \frac{N_p \pi r_p^4}{\Delta x 8\eta}. \tag{8}$$

Curry and Michel (1980) used the expression of Anderson and Malone (1974) and Anderson (1981) to estimate the reflection coeffieient, i.e.,

$$\sigma = (1 - K)^2, \tag{9}$$

where K is the partition coefficient of the solute between the bulk solution and the pore. Eq. 9 was shown by Anderson (1981) to be theoretically valid for a variety of pore geometries subject to a number of assumptions, where K is calculated using $(1 - a/r_p)^2$. However, he points out that the derivation of Eq. 9 assumes "... the pores have a capillary structure, rather than say, a fibrous mat of very high void fraction" and that at present no corresponding expression exists for fiber-matrix membranes. Idol and Anderson (1986) have shown experimentally that for poly(styrene sulfate) membranes the experimental data for the reflection coefficient does not fit the "hard sphere" cylindrical-pore model from which Eq. 9 is derived. A similar lack of fit is seen in polymer reverse-osmosis membranes, where given the size of the pores, Eq. 9 does not predict the almost perfect solute rejection that is observed (Wiggins, 1988). Curry (1980) accurately estimated reflection coefficients in cellophane and wet gel membranes using Eq. 9, however, the coefficients for small radii solutes in Visking cellulose membranes were substantially underestimated. As Idol and Anderson (1986) point out, the problem with applying Eq. 9 to a fiber-matrix or a microporous membrane is not entirely due to the inapplicability of Eq. 9, but to the use of either Eq. 2 or the term $(1 - a/r_p)^2$ to predict the partition coefficient. Both estimate the partition coefficient from strictly steric influences but do not take into account the exclusion (or inclusion) of the solute from the membrane by chemical or solvation effects. Mardsen (1985), Ling (1987), and Browne et al. (1982) have all shown that in highly water-swollen matrix gels, the partition coefficients of low molecular weight solutes are not predictable from Eq. 2. For example, the partition of sugars increases the more highly swollen the matrix becomes (Mardsen, 1965; Ling, 1987), a result opposite to that predicted by Eq. 2.

In spite of the lack of an appropriate expression for the reflection coefficients, Eqs. 5 and 7 have been shown to provide a quantitative and consistent description of the hydrostatic flow and solute diffusion through fiber-matrix membranes, including a number of different types of capillary endothelium and water-swollen polymer membranes.

Eq. 7 predicts that the hydraulic permeability of a membrane will approach infinity as the void fraction, ϵ, approaches unity and Yasuda et al. (1971) have shown that the value of the hydraulic permeability does increase exponentially as the void fraction approaches 1.0 in artificial water-swollen polymer membranes. This cannot occur in epithelial membranes because friction with the walls of the "macropore" limits the hydraulic permeability (Idol and Anderson, 1986).

All calculations were solved on a VAX 750 computer, in double precision, with the C programming language. Plots were generated with the AT&T S graphics package.

RESULTS

Evaluation of the Transport Parameters

Artificial membranes. Before examining the application of the fiber-matrix model to the proximal tubule we tested its applicability to aritficial membranes to see if we could generate a set of transport parameters that are close to the experimentally determined values. Curry (1980) undertook a similar analysis and generally obtained a good fit between experimental data and the fiber-matrix model. Tables I and II are the results from applying the fiber-matrix and the pore models to a Sylvania wet gel membrane and Visking dialysis tubing. The fiber-matrix hydraulic permeability coefficient was calculated from Eq. 7. To calculate the hydraulic permeability we required values for the void fraction, ϵ, the radius of the fibers making up the structure of the membrane, the area of the membrane, and the thickness of the membrane. In both cases the fiber radius we chose was 6.0×10^{-8} cm because this is similar to the fiber radius of methyl cellulose (Ogston et al., 1973). The thickness of the membrane was taken from the work of Ginzburg and Katchalsky (1963). The fractional area of the membrane was 1.0 since in both cases the membranes under study by Ginzburg and Katchalsky were a single homogeneous phase. The viscosity-term, η, is the same as that for water at 25°C. The value of ϵ is a function of the fiber radius r_f and the fiber length per unit volume of fiber matrix, l. Since we had a good estimate of r_f, the only remaining unknown was l. We therefore chose to use l as a fitting parameter, adjusting its value, and as result the value of ϵ, until our predicted value of the hydraulic permeability matched the experimental values given by Ginzburg and Katchalsky (1963). The permeabilities and reflection coefficients of glucose, sucrose, and urea were then calculated using Eqs. 5 and 9. To calculate the permeability coefficients the only additional parameters required were the solute diffusivities. Eqs. 6 and 8 were used to calculate the solute and hydraulic permeabilities of the membranes according to the pore model. The pore radius (r_p) was adjusted to account for the measured hydraulic permeability and the solute permeabilities and reflection coeffieients were then calculated assuming this pore radius.

TABLE I

Calculated and Experimental Values for L_p, P_s, and σ. Sylvania Wet Gel Membrane

Solute	Diffusivity	Molecular radius	P_s (fiber)	P_s (pore)	P_s (exp)	σ (fiber)	σ (pore)	σ (exp)
	$\times 10^5\ cm^2 \cdot s^{-1}$	*nm*	$\times 10^5\ cm \cdot s^{-1}$	$\times 10^5\ cm \cdot s^{-1}$	$\times 10^5\ cm \cdot s^{-1}$			
Sucrose	0.70*	0.45*	34.2	55.0	51.5‡	0.054	0.035	0.036‡
Glucose	0.91*	0.36*	50.0	78.5	82.1‡	0.033	0.022	0.024‡
Urea	1.20*	0.26*	74.7	113.8	212.7‡	0.016	0.001	0.024‡
L_p, $cm \cdot s^{-1}\ (cm\ H_2O)^{-1}$	9.6×10^{-8}	Fiber-matrix model						
L_p, $cm \cdot s^{-1}\ (cm\ H_2O)^{-1}$	9.6×10^{-8}	Pore model						
L_p, $cm \cdot s^{-1}\ (cm\ H_2O)^{-1}$	9.6×10^{-8}	Experimental‡						

The hydraulic permeability coefficients were calculated from Eqs. 7 and 8. The solute permeability coefficients were calculated from Eqs. 5 and 6. The reflection coefficients were determined from Eq. 9, using Eq. 2 to calculate the partition coefficient for the fiber-matrix model and the expression $(1 - a/r_p)^2$ for the pore model. A_f is 1.0. Δx is 8.4×10^{-5} cm, r_f is 6.0×10^{-8} cm, r_p is 2.42×10^{-7} cm, η is 9.07×10^{-6}, and κ is 5. The value of ϵ giving the best fit to the data is 0.872. The estimated void fraction, for a water content of 0.77 (Ginzburg and Katchalsky, 1963) (assuming a partial molar volume of 0.68 for the gel fibers) is 0.84.

*Ullrich, 1973.

‡The experimental values for the permeabilities and hydraulic permeability coefficient, and the reflection coefficients are from Ginzburg and Katchalsky (1963). The thickness of the membrane was measured by Ginzburg and Katchalsky (1963).

TABLE II

Calculated and Experimental Values for L_p, P_s, and σ. Visking Dialysis Tubing

Solute	Diffusivity	Molecular radius	P_s (fiber)	P_s (pore)	P_s (exp)	σ (fiber)	σ (pore)	σ (exp)
	$\times 10^5$ cm^2·s^{-1}	nm	$\times 10^5$ cm·s^{-1}	$\times 10^5$ cm·s^{-1}	$\times 10^5$ cm·s^{-1}			
Sucrose	0.70*	0.45*	64.2	114.1	39.2‡	0.053	0.021	0.16‡
Glucose	0.91*	0.36*	93.8	158.4	71.8‡	0.032	0.020	0.12‡
Urea	1.20*	0.26*	140.0	224.3	200.8‡	0.016	0.007	0.01‡

L_p, cm·s^{-1} (cm H_2O)$^{-1}$	3.01×10^{-7}	Fiber-matrix model
L_p, cm·s^{-1} (cm H_2O)$^{-1}$	3.04×10^{-7}	Pore model
L_p, cm·s^{-1} (cm H_2O)$^{-1}$	3.04×10^{-7}	Experimental‡

The hydraulic permeability coefficients were calculated from Eqs. 7 and 8. The solute permeability coefficients were calculated from Eqs. 5 and 6. The reflection coefficients were determined from Eq. 9, using Eq. 2 to calculate the partition coefficient for the fiber-matrix model and the expression $(1 - a/r_p)^2$ for the pore model. A_f is 1.0. Δx is 4.5×10^{-3} cm, r_f is 6.0×10^{-8} cm, r_p is 3.13×10^{-7} cm, η is 9.07×10^{-6}, and κ is 5. The value of ϵ is 0.873. The estimated void fraction, for a water content of 0.68 (Ginzburg and Katchalsky, 1963) (assuming a partial molar volume of 0.68 for the gel fibers) is 0.78.

*Ullrich, 1973.

‡The experimental values for the permeabilities and hydraulic permeability coefficient, and the reflection coefficients are from Ginzburg and Katchalsky (1963). The thickness of the membrane Δx was measured by Ginzburg and Katchalsky (1963).

The reflection coefficients for the pore case were determined from Eq. 9, using the expression $(1 - a/r_p)^2$ for the partition coefficient.

For the Sylvania wet gel membrane (Table I) both the pore and fiber-matrix models provide reasonable estimates of the sucrose and solute permeabilities and reflection coefficients once the hydraulic permeability has been matched to the experimental values. The estimated values of the urea permeabilities were not as close to the measured values. However, urea, because of its structure (Shieh and Lyman, 1979), may break the bound water structure within the hydrophilic regions, and thus pass more readily through the membrane, be it pore or fiber matrix. More importantly, the results for the Visking dialysis membrane shown in Table II illustrate the major problem with the application of the pore model in membrane transport studies. The predicted permeabilities for glucose and sucrose are three and two times greater than the experimental values. To accurately (i.e., to within a few percent) fit the solute permeability data to the pore model, pore radii one-third of that required to fit the hydraulic permeability are needed. Reduction of pore radii to account for the measured solute permeabilities would lead to a predicted hydraulic permeability an order of magnitude smaller than that measured. In other words, one cannot calculate pore radii from solute permeability data to estimate the hydraulic permeability of a particular membrane, a fact which has been demonstrated in other membranes (Maroudas, 1970; Yasuda et al., 1971; Curry and Michel, 1980; Idol and Anderson, 1986). Thus the approach taken by Preisig and Berry (1985) is not valid. It should be noted, however, that this applies to the fiber-matrix model as well, i.e., the void fraction cannot be estimated from the solute permeability, even though a particular void fraction can fit both solute and hydraulic permeability data.

Tight Junction Epithlium

The flow across tubular epithelium has been extensively modeled by others, but as stated in the introduction there is considerable controversy as to the role of the tight junction in accounting for both solute and volume flow. We wished to investigate whether or not the tight junction could account for the observed permeabilities of the entire tubule epithelium.

To model the flow through the tight junction of proximal tubules several input parameters were required for the model equations. The viscosity η is that of water at 37°C, the fractional area of the membrane composed of the tight junction was taken to be 0.005% similar to that used in other models of the proximal tubule (Weinstein, 1982; Preisig and Boony, 1985). The values of a and D_0 are chosen from the literature and are given in Tables III and IV. The value of κ is 2, the value determined by Adamson and Curry (1982) for hyaluronic acid gels. The value of r_f was chosen to be similar to the fiber radii of hyaluronic acid (5.9×10^{-8} cm) and sulfated proteoglycans (5.1×10^{-8} cm) (Ogston et al., 1973), which are components of the loose intercellular mesh and would be expected to be of similar radius as the fibrous proteins making up the strands of the tight junction that one observes in freeze-fracture studies. It is important to note that the tight junction molecular structure at the microscopic level, at which the fiber-matrix model is applicable, is not comparable to the morphology observed using freeze-fracture techniques. We are applying the

TABLE III

Calculated and Experimental Values for L_p, and P_s. Proximal Convoluted Tubule of the Rat

Solute	Diffusivity	Molecular radius	P_s (fiber)	P_s (exp)
	$\times 10^5$ $cm^2 \cdot s^{-1}$	*nm*	$\times 10^5$ $cm \cdot s^{-1}$	$\times 10^5$ $cm \cdot s^{-1}$
Mannitol	0.673*	0.40*	1.2	1.5*
Sucrose	0.521*	0.45*	0.92	—
Raffinose	0.458*	0.60*	0.78	‡
Inulin	0.130*	1.50*	0.15	‡
Na^+	1.78§	0.36‖	3.3	21.1¶
Cl^-	2.72§	0.18‖	5.6	32.3¶
L_p, $cm \cdot s^{-1}$ $(cm\ H_2O)^{-1}$	1.60×10^{-7}	Fiber-matrix model		
L_p, $cm \cdot s^{-1}$ $(cm\ H_2O)^{-1}$	1.64×10^{-7}	Experimental*		

The hydraulic permeability coefficient was calculated from Eq. 7. The solute permeability coefficients were calculated from Eq. 5. A_f is 5.0×10^{-5}, Δx is 2.0×10^{-5} cm, r_f is 8.0×10^{-8} cm, the water viscosity is 9.16×10^{-6}, and κ is 2. The calculated value of ϵ was 0.965.

*Ullrich, 1973.

‡No detectable permeability.

§Renkin and Curry, 1979.

‖Schafer and Andreoli, 1979*a*.

¶Frömter et al., 1973.

fiber-matrix model to the molecular structure within the strand (or o-ring) and not to the collection of strands one observes with freeze-fracture. In our model, an increased number of strands is equivalent to an increased tight junction thickness. The value of ϵ was adjusted in the same manner as that used to fit the data of the artificial membranes, i.e., by adjusting the length l of fibers per unit volume of mesh.

TABLE IV

Calculated and Experimental Values for L_p, and P_s. Proximal Convoluted Tubule of the Rabbit

Solute	Diffusivity	Molecular radius	P_s (fiber)	P_s (exp)
	$\times 10^5$ $cm^2 \cdot s^{-1}$	*nm*	$\times 10^5$ $cm \cdot s^{-1}$	$\times 10^5$ $cm \cdot s^{-1}$
Mannitol	0.673*	0.40*	1.3	—
Sucrose	0.521*	0.45*	0.96	0.69‡
Raffinose	0.458*	0.60*	0.80	—
Inulin	0.130*	1.50*	0.16	—
Na^+	1.78§	0.36‖	3.4	2.3¶
Cl^-	2.72§	0.18‖	5.4	2.6–5.6‖
L_p, $cm \cdot s^{-1}$ $(cmH_2O)^{-1}$	2.40×10^{-7}	Fiber-matrix model		
L_p, $cm \cdot s^{-1}$ $(cmH_2O)^{-1}$	2.45×10^{-7}	Experimental data‡		

The hydraulic permeability coefficient was calculated from Eq. 7. The solute permeability coefficients were calculated from Eq. 5. A_f is 5.0×10^{-5}, Δx is 2.0×10^{-5} cm, r_f is 8.0×10^{-8} cm, the water viscosity is 9.06×10^{-6}, and κ is 2. The calculated value of ϵ was 0.971.

*Ullrich, 1973.

‡Schafer and Andreoli, 1979*b*.

§Renkin and Curry, 1979.

‖Value for NaCl from Schafer and Andreoli, 1979*a*.

¶Holmberg et al., 1981.

In the cases discussed we have ignored the role of the lateral intercellular space in providing a significant barrier to either solute diffusion or volume flow. If one calculates the hydraulic permeability of the lateral intercellular space, using a pore model and realistic estimates of the fractional area of the lateral intercellular space and the epithelial thickness, the hydraulic permeabilities are an order of magnitude greater than those measured in the epithelial membranes (Berry, 1983). A similar calculation for the solutes indicates that the permeability of the lateral intercellular spaces is an order of magnitude greater than the epithelial values (Schafer and Andreoli, 1979*a*). Since the tight junction and lateral intercellular space are series resistances, there would have to be at least an order of magnitude decrease in the solute and hydraulic permeabilities of the lateral intercellular spaces before a detectable effect on the total epithelial permeability could be observed. It is therefore unlikely that the lateral intercellular space provides significant resistance to flow or is a significant factor in regulating transport.

The restriction imposed on the hydraulic permeability by the walls of the "macropores" containing the fiber-matrix structure will also be insignificant for "macropore" radii >70 Å.

For the fiber-matrix model it can be seen that there is good agreement between the calculated and observed value of the hydraulic conductivity, L_p, and the permeability coefficients, P_s, for those solutes that cross the proximal tubule only via the paracellular pathway (Tables III and IV), especially when one examines the range of experimental values from which the reported mean values are derived. It also predicts values for the permeability coefficients of Cl and Na close to the experimental values observed in the rabbit proximal tubule (Table IV), which is in agreement with the belief that the passive ion transport involves an extracellular route (Schafer and Andreoli, 1979*b*). For the rat tubule, the predicted ion permeabilities are similar to mannitol, but an order of magnitude less than the observed permeabilities, indicating that the transcellular ion permeability may be significant. This is at odds with the belief that passive ion transport is exclusively via the paracellular pathway in the rat proximal tubule (Frömter, 1979). However, it would explain the order of magnitude difference between the ion and mannitol permeabilities.

As discussed earlier, the use of both Eq. 9 and Eq. 2 to predict the reflection coefficients is highly questionable for a high-void fraction fiber-matrix membrane (Anderson, 1981). This was experimentally shown by Idol and Anderson (1986) who developed a physical model of a tight junctional structure filled with a polymer mesh. They formed high void-fraction fiber-matrix membranes of poly(styrene sulfate) in large pores (29–140 nm) track-etched in mica membranes. They then compared the hydraulic permeabilities and the thiourea solute permeabilities of the pores with and without the polymer mesh. In addition, they measured the sieving coefficient for thiourea in some of the polymer-filled pores. We applied Eq. 7 and Eq. 8 to Idol and Anderson's data on the reduction of hydraulic permeability due to the presence of the polymer mesh to estimate the void fraction of the three pores of their Table IV. The void fraction values were calculated by setting the ratio of Eqs. 7 and 8 equal to the reduction in the measured hydraulic permeability due to the presence of the polymer mesh, and solving for the corresponding values of ϵ. Eq. 7 was multiplied by 0.68 to correct for the noncircular cross section of the pore. The

total membrane area was set equal to unity by making A_f equal to one in Eq. 7, and adjusting the number of pores, N_p, in Eq. 8. Fig. 1 is a plot of the measured reflection coefficient against the calculated void fractions. The reflection coefficients and the hydraulic permeability data are taken from Table IV of Idol and Anderson (1986). The reflection coefficients predicted from Eqs. 2 and 9 for these void fractions were all $\ll 0.1$, whereas the measured reflection coefficients range from 0.16 to 0.49. Similarly, application of Eqs. 2 and 9 to the tight junction predicts reflection coefficients $\ll 0.1$, whereas the reported values for the solutes in Tables III and IV range from 0.5 to 1.0. Given that the tight junction is a complex glycoprotein structure, that Eq. 2 ignores all but the steric interactions between solute and fibers, and that there is no formal justification for using Eq. 9 where a fiber matrix is assumed, it is apparent that Eqs. 2 and 9 cannot accurately predict the reflection coefficients of actual junctional membranes. The formal development and testing of an expression for the reflection coefficient in fiber-matrix membranes is still required (Anderson, 1981), therefore we have not included the reflection coefficients in Tables III and IV.

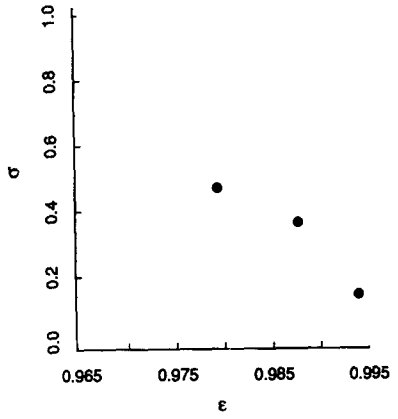

FIGURE 1. A plot of the measured values of the reflection coefficient of thiourea against the void fraction of a polymer mesh membrane. The reflection coefficients are taken from Table IV of Idol and Anderson (1986). The void fraction values were calculated by setting the ratio of Eq. 7 and Eq. 8 equal to the reduction in the measured hydraulic permeability due to the presence of the polymer mesh, and solving for the corresponding value of ϵ. Eq. 7 was multiplied by 0.68 to correct for the noncircular cross section of the pore.

The calculated void fractions for the tubule tight junctions, 0.965 and 0.971, may appear to be extremely high, however, they are less than that of the hyaluronic acid gel studied by Adamson and Curry (1982) ($\epsilon = 0.987$).

The predictions of the fiber-matrix and pore models were directly compared by plotting the ratio of the hydraulic and solute permeability coefficients over the full range of the void fraction and over a wide range of pore radii. Fig. 2 is a plot of the L_p/P_s ratio vs. the void fraction (fiber-matrix model) and the pore radius (pore model). The most important feature of this plot is that for the physiologically relevant ranges of radii and void fraction, the hydraulic permeability relative to the solute permeability is 10- to 100-fold greater with the fiber-matrix model. Fig. 2 indicates why the pore model cannot account for both the hydraulic permeability and the observed solute permeability of the proximal tubule. For the pore model to fit the mannitol and hydraulic permeability data for the rat proximal tubule the L_p/P_s ratio must be $\sim 1.5 \times 10^{-2}$ (*dashed line* in Fig. 2), a value for which the mannitol curve (C) of the pore model does not approach for any physiologically realistic pore

radii. The mannitol curve (*C*) for the fiber-matrix model reaches this value at a void fraction of ~0.98.

Another relevant feature of the fiber-matrix membrane model is that solute permeability is a function of the void fraction over the entire range of possible values, even at very high void fractions. Such a dependency of solute permeability on void fraction has been observed by Ito (1961) for oxygen, nitrogen, and carbon dioxide transport through poly(vinyl alcohol) and cellophane membranes. The permeability of the smaller solutes is independent of pore radii except for pores of dimensions similar to the solutes, in which case the interaction between the walls of the pore and the solute must be taken into account (see Pappenheimer, 1951).

Fig. 2 also shows why we did not use the solute permeability as the fitting parameter to estimate the void fraction of the proximal tubules of Tables III and IV, and

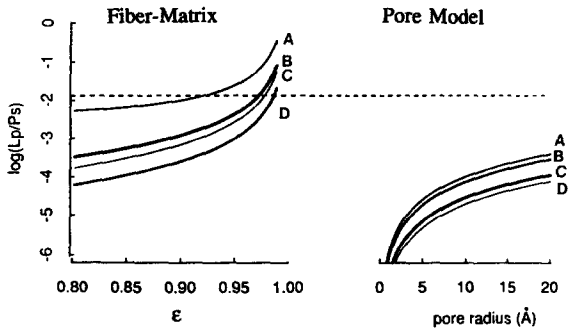

FIGURE 2. A plot of the calculated hydraulic permeability L_p ($cm \cdot s^{-1}$) divided by the calculated solute permeability Ps($cm \cdot s^{W1}$) against the fiber-matrix void fraction and pore radius, for inulin (curve *A*), raffinose (curve *B*), mannitol (curve *C*), and sodium (curve *D*). The hydraulic and solute permeabilities as a function of the void fraction were calculated with Eqs. 5 and 7. The hydraulic permeability and the solute permeabilities as a function of pore radii were calculated with Eqs. 6 and 8, with $A_f = N_p \pi r_p^2$, and $(1 - a/r_p)$ assumed to be unity. The solute diffusivities and molecular radii are those given in Table III.

then estimate the hydraulic permeabilities. Because the solute permeability does not vary as much as the hydraulic permeability with changes in void fraction, a reasonable fit to mannitol, NaCl, or sucrose permeability can be made with void fractions ranging from <0.90 all the way to 1.0. The predicted values of L_p would then range over several orders of magnitude. Just as in the case of the pore model, it is inappropriate to use a solute permeability to estimate a hydraulic permeability.

Application of the Fiber-Matrix Model to Reabsorption from the Proximal Tubule

A model describing salt and volume reabsorption from the rat proximal tubule has been developed by Weinstein (1984). The model incorporates neutral active salt transport and passive reabsorptive forces due to asymmetrical salt solutions and oncotic and hydrostatic pressures. His model includes the cell membrane transport

coefficients (L_{cell}, P_{cell}, σ_{cell}), as well as the transport coefficients of the basement membrane (L_{bm}, P_{bm}, σ_{bm}), and the tight junction (L_{tj}, P_{tj}, σ_{tj}). The model allows the values of L_{tj}, P_{tj}, and σ_{tj}, predicted from the fiber-matrix model, to be directly inserted into the volume-flow equation developed by Weinstein, and the response of the tubule to changes in the void fraction to be examined. We have replaced the transport coefficients chosen by Weinstein for the tight junction by those calculated using the fiber-matrix model, but we have adopted his values for the transport coefficients of the cell and basement membranes including the large transcellular hydraulic permeability. It should be noted that Weinstein's chosen value for the cell membrane hydraulic permeability was 4.3×10^{-7} cm$^3 \cdot$s^{-1} mmHg$\cdot$cm^{-2}, 2.6 times the value predicted by the tight junction model at a void fraction of 0.965 (Table III) and larger than that reported for proximal tubule epithelium (Tables III and IV).

The equation derived by Weinstein for the volume reabsorption from the rat proximal tubule is

$$J_v = L_p[\pi_s - \pi_{lum} + RT\sigma(C_s - C_{lum}) + RT\sigma\hat{C}]. \tag{10}$$

L_p and σ are composite transport coefficients incorporating the cell, basement, and tight junctional hydraulic and salt permeabilities and reflection coefficients, i.e.,

$$L_p = \frac{L_{epit}(P_{lum} + P_{bm})}{P_{lum} + P_{bm} + RTL_{epit}\sigma_{lum}^2 C_0}, \tag{11}$$

$$\sigma = \frac{P_{bm}\sigma_{lum}}{P_{lum} + P_{bm}}, \tag{12}$$

with

$$L_{epit} = \frac{L_{lum}L_{bm}}{L_{lum} + L_{bm}}, \tag{13}$$

$$L_{lum} = L_{tj} + L_{cell}, \tag{14}$$

$$P_{lum} = P_{tj} + P_{cell} + (\sigma_{tj} - \sigma_{cell})^2 \, RTC_o \frac{L_{tj}L_{cell}}{L_{tj} + L_{cell}}, \tag{15}$$

and

$$\sigma_{lum} = \frac{L_{cell}\sigma_{cell} + L_{tj}\sigma_{tj}}{L_{cell} + L_{tj}}. \tag{16}$$

C_{lum} is the luminal salt concentration, C_s is the peritubular salt concentration, π_{lum} is the luminal oncotic concentration, C_o is a reference osmolality, π_s is the peritubular oncotic concentration, and $\hat{C}$ is the active transport coefficient.

As part of his study Weinstein (1984) investigated the effects of varying the oncotic and active driving forces on the reabsorption, with a fixed set of transport coefficients. To investigate the effect of tight junction structure on the volume reabsorption, we varied void fraction under four different conditions (Fig. 3). Curve *A* is for active transport, with an isotonic luminal perfusate and a 5 mOsmol oncotic gradient due to an impermeant solute on the peritubular side of the epithelium,

curve *B* is for active transport with a 2 mOsmol hypotonic luminal perfusate, curve *C* is for active transport with an isotonic luminal perfusate, and curve *D* is for active transport with a 2 mOsmol hypertonic luminal perfusate.

A void fraction of 0.98, close to the values used in Tables III and IV, predicts a volume flux of ~60 nl·cm^{-2}·s^{-1} for active transport with an isotonic luminal perfusate, essentially identical to that measured in proximal convoluted tubule of the rat (Schafer and Andreoli, 1979*a*). Varying the void fraction over the range of 0.97–0.99 results in a 50–75% change in volume reabsorption, depending on the driving forces responsible, indicating that net fluid reabsorption could be significantly influenced by small variations in tight junction void fractions no matter what the nature of the driving force. At high void fractions (>0.99) the reabsorption will essentially cease as a result of the increased permeability of salt and/or water

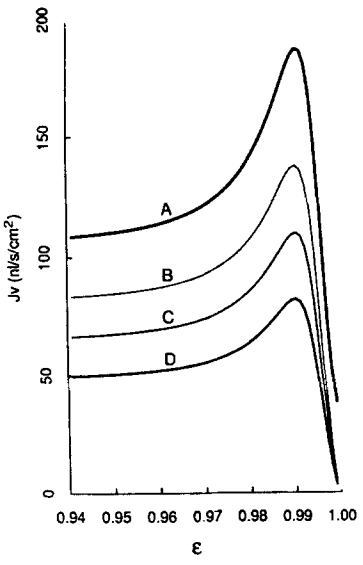

FIGURE 3. Steady-state volume reabsorption from rat proximal tubule as a function of the void fraction, ϵ. The curves were calculated from Eqs. 10–16. The values of L_{tj}, P_{tj}, and σ_{tj}, were calculated from Eqs. 5, 7, and 9 as for Tables III and IV. The values of the other parameters were taken from Weinstein (1984). $L_{cell} = 4.3 \times 10^{-7}$ cm^3·s^{-1} mmHg·cm^{-2}, $L_{bm} = 6.7 \times 10^{-6}$ cm^3·s^{-1} mmHg·cm^{-2}, $P_{cell} = 3.1 \times 10^{-10}$ cm·s^{-1}, $P_{bm} = 11.7 \times 10^{-4}$ cm·s^{-1}, $\sigma_{cell} = 1.0$, $\sigma_{bm} = 0.0$, $\hat{C} = 1.6 \times 10^{-2}$ mmol, $C_o = 290$ mOsmol. Curve *A* is for active transport, with an isotonic luminal perfusate and a 5 mOsmol oncotic gradient due to an impermeant on the peritubular side of the epithelium, curve *B* is for active transport with a 2 mOsmol hypotonic luminal perfusate, curve *C* is for active transport with an isotonic luminal perfusate, and curve *D* is for active transport with a 2 mOsmol hypertonic luminal perfusate.

through the tight junction, and the corresponding diffusive or convective backflux. Under such conditions the active transport cannot generate a salt gradient to drive the overall volume reabsorption.

DISCUSSION

We have shown that a fiber-matrix model for membrane transport fits measurements made with both artificial membranes and the proximal tubule epithelium. The ability of the fiber-matrix model to represent the proximal tubule data does not prove that the majority of volume flow across the proximal epithelium occurs via the tight junction only that the tight junction is capable of allowing for such a flow. As Diamond (1979) has pointed out, the arguments as to the route of transepithelial

volume cannot be resolved with current experimental techniques. The measurement of cell membrane and transepithelial hydraulic permeability are performed by imposing osmotic gradients across the epithelium and monitoring the volume flow. However, the true osmotic gradient existing across the epithelium is a function of the unstirred diffusion layers at the membrane surfaces. In the absence of knowledge of diffusional and polarization delays or resolution of osmotic transients in the renal tubules, one cannot determine the true osmotic gradients, therefore no accurate calculation of the hydraulic permeability coefficient is possible.

The major consequence of a tight junction transport conforming to a model as we have proposed is that subtle changes in the structure of the tight junction could change both hydraulic and solute permeability, thereby providing a mechanism for precise control of epithelial transport driven by both active and passive mechanisms.

The fiber-matrix model has been applied to model flow only across the tight junctional structure of the kidney nephron. Application of the model to transport across other epithelial membranes especially the kidney glomerulus is warranted. The fiber-matrix model is an attractive model to apply to the cell membranes since it can explain the high hydraulic permeability of these membranes, without the necessity of large porous structures. The lipid-protein cell membranes and the cellular cytoplasm are both examples of fiber-mesh/gel membranes and the application of the fiber-matrix model flow equations may be appropriate. Any change in the hydration state and/or structure (i.e., void fraction) of the cell membranes or the cytoplasma would be expected to have a dramatic effect on transcellular permeabilities. Ionic composition, chelators, and proteins in solutions could modify the permeability of membranes to water and solutes. Especially interesting is the possibility that changes in the osmotic pressure could directly regulate the void fraction, as has been observed in biological, fiber-mesh gels (Douzou, 1987). Changes in ionic strength and, as a result, differences in the void fraction of the tight junction, could explain differences in the permeability of superficial and deep nephrons and differences between convoluted and pars recta tubules.

This work was supported by the Medical Research Council of Canada, the Kidney Foundation of Canada, and the Defence and Civil Institute of Environmental Medicine, Downsview, Ontario.

We wish to thank Dr. D. Welling and the reviewers for their valuable comments.

Original version received 10 May 1988 and accepted version received 26 April 1989.

REFERENCES

Adamson, R. H., and F. E. Curry. 1982. Water flow through a fiber matrix of hyaluronic acid. *Microvascular Research.* 23:239. (Abstr.)

Anderson, J. L. 1981. Configurational effect on the reflection coefficient for rigid solutes in capillary pores. *Journal of Theoretical Biology.* 90:405–426.

Anderson, J. L., and D. M. Malone. 1974. Mechanism of osmotic flow in porous membranes. *Biophysical Journal.* 14:957–982.

Bear, J. 1972. Dynamics of Fluids in Porous Media. Elsevier, Amsterdam. 157–159.

Berry, C. A. 1983. Water permeability and pathways on the proximal tubule. *American Journal of Physiology.* 245:F279–F294.

Browne, C. L., A. H. Lockwood, and A. Steiner. 1982. Localization of the regulatory subunit of type II cyclic AMP-dependent protein kinase on the cytoplasmic microtubule of cultured cells. *Cell Biology International Reports.* 6:19–28.

Carman, P. C. 1937. Fluid flow through granular beds. *Transactions of the Institute of Chemical Engineering.* 15:150.

Curry, F. E. 1980. Is the transport of hydrophilic substances across the capillary wall determined by a network of fibrous molecules. *Physiologist.* 23:90–93.

Curry, F. E. 1984. Mechanics and thermodynamics of transcapillary exchange. *In* Handbook of Physiology. Section 2. Vol. IV. Microcirculation, Part 1. American Physiological Society, Bethesda, MD. 309–374.

Curry, F. E., and A. E. Michel. 1980. A fiber matrix model of capillary permeability. *Microvascular Research.* 20:96–99.

Diamond, J. M. 1979. Osmotic water flow in leaky epithelia. *Journal of Membrane Biology.* 51:195–216.

Douzou, P. 1987. Biological macromolecules as gels: Functional similarities. *Proceedings of the National Academy of Sciences.* 84:6741–6744.

Frömter, E. 1979. Solute transport across epithelium: what can we learn from micropuncture studies on kidney tubules. *Journal of Physiology.* 288:1–39.

Frömter, E., G. Rumrich, and K. J. Ullrich. 1973. Phenomenological description of Na^+, Cl^-, and HCO_3^- absorption from proximal tubules of the rat kidney. *Pflügers Archiv.* 343:189–220.

Ginzburg, B. Z., and A. Katchalsky. 1963. The frictional coefficients of the flows of non-electrolytes through artificial membranes. *Journal of General Physiology.* 47:403–418.

Griepp, E. B., W. J. Dolan, E. S. Robbins, and D. D. Sabatini. 1983. Participation of plasma membrane proteins in the formation of tight junctions by cultured epithelial cells. *Journal of Cellular Biology.* 96:693–702.

Gumbiner, B. 1987. Structure, biochemistry, and assembly of epithelial tight junctions. *American Journal of Physiology.* 253:C749–C758.

Hayward, A. F., and M. Hackemann. 1973. Electron microscopy of membrane coating granules and a cell surface in keratinized and non-keratinized human oral epithelium. *Journal of Ultrastructural Research.* 43:205–219.

Holmberg, C., J. P. Kokko, and H. R. Jacobson. 1981. Determination of chloride and bicarbonate permeabilities in proximal convoluted tubules. *American Journal of Physiology.* 241:F386–F394.

Idol, W. K., and J. L. Anderson. 1986. Effects of adsorbed polyelectrolytes on convective flow and diffusion in porous membranes. *Journal of Membrane Science.* 28:269–286.

Ito, Y. 1961. Permeability of gases and vapours through high-polymer films. XIV. The permeability of gases through moistened high-polymer films. *Kobunshii Kagaku.* 18:158–163.

Kozeny, J. 1927. Ober Kapillare Leitung des Wassers in Boden. *Kolloid Zeitung.* 136:29–43.

Leenaars, A. F., and A. J. Burggraaf. 1985. The preparation and characterization of aluminae membranes with ultrafine pores. *Journal of Membrane Science.* 24:245–260.

Ling, G. N. 1987. Studies of the physical state of water in living cells and model systems. VII. Exclusion of sugars and sugar alcohols from the water in sulfonate ion exchange resins: the "size rule". *Physiological Chemistry and Physics and Medical NMR.* 19:193–198.

Mardsen, N. V. B. 1965. Solute behavior in tightly cross-linked dextran gels. *Annals of the New York Academy of Sciences.* 125:428–457.

Maroudas, A. 1970. Distribution and diffusion of solutes in articular cartilage. *Biophysical Journal.* 10:365–379.

Massey, B. S. 1983. *Mechanics of Fluids.* Van Nostrand Reinhold, Wokingham, England. 203 pp.

Ogston, A. G., B. N. Preston, and J. D. Wells. 1973. On the transport of compact particles through solutions of chain polymers. *Proceedings of the Royal Society of London* A333:297–316.

Oschman, J. L. 1978. Morphological correlates of transport. *In* Transport Across Multi-Membrane Systems. G. Giebisch, editor. Springer-Verlag, New York. 55–93.

Pappenheimer, J. R., E. M. Renkin, and L. M. Borrero. 1951. Filtration, diffusion, and molecular sieving through peripheral capillary membranes. *American Journal of Physiology.* 167:13–46.

Preisig, P. A., and C. A. Berry. 1985. Evidence for transcellular osmotic water flow in rat proximal tubules. *American Journal of Physiology.* 249:F124–F131.

Renkin, E. M., and F. E. Curry. 1979. Transport of water and solutes across capillary endothelium. *In* Transport Organs. G. Giebisch, editor. Springer-Verlag, Berlin. 1–45.

Schafer, J. A., and T. E. Andreoli. 1979*a*. Rheogenic and passive Na^+ reabsorption by the proximal tubule. *Annual Reviews of Physiology.* 41:211–217.

Schafer, J. A., and T. E. Andreoli. 1979*b*. Perfusion of isolated mammalian renal tubules. *In* Transport Organs. G. Giebisch, editor. Springer-Verlag, New York. 473–517.

Shieh, D. F., and D. J. Lyman. 1979. The role of partitioning and diffusivity of non-electrolyte solutes in membrane permeabilities of block-copolyether-esters. *Journal of Membrane Science.* 5:305–318.

Ullrich, K. J. 1973. Permeability characteristics of the mammalian nephron. *In* Handbook of Physiology. Renal Physiology. J. Orloff and R. W. Berliner, editors. American Physiological Society, Bethesda, MD. 377–414.

Weinstein, A. M. 1982. Nonequilibrium thermodynamic model of the rat proximal tubule epithelium. *Biophysical Journal.* 22:153–170.

Weinstein, A. M. 1984. Transport by epithelia with compliant lateral intercellular spaces: asymmetric oncotic effects across the rat proximal tubule. *American Journal of Physiology.* 247:F848–F862.

Wiggins, P. M. 1988. Water structure in polymer membranes. *Progress in Polymer Science.* 13:1–35.

Yasuda, H., C. E. Lamaze, and A. Peterlin. 1971. Diffusion and hydraulic permeability of water in water swollen polymer membranes. *Journal of Polymer Science.* A:1117–1131.